ORIGINAL ARTICLE–PHYSICS & ENGINEERING

Optimizing irradiation conditions for low-intensity pulsed ultrasound to upregulate endothelial nitric oxide synthase

Daiki Ouchi[1] · Shohei Mori[1] · Mototaka Arakawa[1,2] · Tomohiko Shindo[3] · Hiroaki Shimokawa[4,3] · Satoshi Yasuda[3] · Hiroshi Kanai[1,2]

Abstract

Purpose Here we aimed to develop a minimally invasive treatment for ischemic heart disease and demonstrate that low-intensity pulsed ultrasound (LIPUS) therapy improves myocardial ischemia by promoting myocardial angiogenesis in a porcine model of chronic myocardial ischemia. Studies to date determined the optimal treatment conditions within the range of settings available with existing ultrasound equipment and did not investigate a wider range of conditions.

Methods We investigated a broad range of five parameters associated with ultrasound irradiation conditions that promote expression of endothelial nitric oxide synthase (eNOS), a key molecule that promotes angiogenesis in human coronary artery endothelial cells (HCAEC).

Results Suboptimal irradiation conditions included 1-MHz ultrasound frequency, 500-kPa sound pressure, 20-min total irradiation time, 32–48-µs pulse duration, and 320-µs pulse repetition time. Furthermore, a proposed index, P_N, calculated as the product of power and the total number of irradiation cycles applied to cells using LIPUS, uniformly revealed the experimental eNOS expression associated with the various values of five parameters under different irradiation conditions.

Conclusion We determined the suboptimal ultrasound irradiation conditions for promoting eNOS expression in HCAEC.

Keywords Low-intensity pulsed ultrasound therapy · Endothelial nitric oxide synthase · Angiogenesis · Human coronary artery endothelial cells

Introduction

Ischemic heart disease (IHD) is the leading cause of death in developed countries [1], and its incidence is increasing in developing countries [2]. Therefore, noninvasive treatment methods for this disorder are needed. Ultrasound has been used clinically for diagnosis, bone therapy, tumor resection, and drug delivery enhancement [3]. Low-intensity pulsed ultrasound (LIPUS) reportedly induced angiogenesis and ameliorated myocardial ischemia in a porcine model of chronic myocardial ischemia [4]. LIPUS has been used to treat various orthopedic, dental, and brain disorders [5–7].

We have been studying noninvasive treatment methods for microcirculatory disorders such as IHD. We have shown that LIPUS irradiation of human umbilical vein endothelial cells with 32 wave cycles significantly increases the mRNA expression of vascular endothelial growth factor (VEGF), with subsequent therapeutic angiogenesis [4]. However, because these irradiation conditions were determined using existing sector probes, conditions such as the frequency, sound pressure, and pulse repetition frequency were not optimized. We found that a signaling pathway mediated by mechanotransduction was involved in the effects of LIPUS [8]. Indeed, LIPUS may induce the distortion of endothelial caveolae [9, 10], which are transmitted into cells, ultimately leading to the upregulation of endothelial nitric oxide

✉ Mototaka Arakawa
  arakawa@tohoku.ac.jp

✉ Hiroshi Kanai
  hiroshi.kanai.e7@tohoku.ac.jp

1 Graduate School of Engineering, Tohoku University, 6-6-05 Aoba, Aramaki, Aoba-Ku, Sendai, Miyagi 980-8579, Japan

2 Graduate School of Biomedical Engineering, Tohoku University, 6-6-05 Aoba, Aramaki, Aoba-Ku, Sendai, Miyagi 980-8579, Japan

3 Department of Cardiovascular Medicine, Tohoku University Graduate School of Medicine, Sendai, Japan

4 Graduate School, International University of Health and Welfare, Narita, Japan

synthase (eNOS) and VEGF with subsequent therapeutic angiogenesis.

The present study aimed to explore ultrasound irradiation conditions that promote eNOS expression in human coronary artery endothelial cells (HCAEC). We varied the total irradiation time, sound pressure, frequency, and pulse repetition frequency, as well as the wave cycle, as discussed in a previous report [4]. We examined the ultrasound irradiation conditions in HCAEC with LIPUS in vitro and used the expression level of eNOS, a key molecule that promotes angiogenesis, to quantitatively evaluate cell activation under the suboptimal LIPUS irradiation conditions. Furthermore, a proposed index, P_N, calculated as the product between power and the total number of irradiation cycles applied to cells using LIPUS, uniformly showed the experimental ultrasound contribution to eNOS expression for the various values of five parameters under different irradiation conditions.

Materials and methods

Cell culture

HCAEC (CC-2585; Lonza, Tokyo, Japan) from one donor were cultured in endothelial cell medium (Lonza). The cells were passaged to passage 2, resuspended 24 h before LIPUS irradiation, sown uniformly in 24-well plates (353,047; Corning, New York, USA) ($n=6$) at 4×10^4 cells/well, and incubated (37°C, 5% CO_2).

Irradiation experiment

Figure 1a shows a schematic of the experimental setup. The desired pulse wave was generated using a signal generator (WF1974; NF, Kanagawa, Japan), amplified using a power amplifier (705,810; Yokogawa, Tokyo, Japan), applied to a disk-shaped ultrasound transducer ($\phi = 20$ mm), and irradiated with ultrasound. Four types of transducers with center frequencies of 0.1, 0.3, 1, and 3 MHz were used. The transducers were glued to circular dishes with a bottom surface thickness of 0.8 mm (150,460; Thermo Fisher Scientific, Waltham, USA). The temperature in the thermostatic chamber was kept at 37°C during the experiment. The cells were irradiated with ultrasound through agar (010–15815; Fujifilm Wako Pure Chemicals, Osaka, Japan) ($n=6$). The difference in propagation attenuation between the agar and culture media was neglected.

As illustrated in Fig. 1b, the five parameters that were monitored under ultrasound irradiation conditions were ultrasound frequency f_0 [Hz], maximum sound pressure P_0 [Pa], total irradiation time T_{ttl} [s], pulse duration ΔT [s], and pulse repetition time PRT [s].

The following three parameters are derived from these five parameters. The wave cycle wl [cycles] was obtained by multiplying the pulse duration ΔT by the frequency f_0, that is, $wl = \Delta T \times f_0$. The duty cycle DC [%] was calculated as the ratio of the pulse duration ΔT to the pulse repetition time PRT, that is, $DC = \Delta T / PRT$. Since the number of irradiations with a pulse repetition time PRT is T_{ttl}/PRT within the total irradiation time T_{ttl}, the effective irradiation time T_{eff} [s] is given by

$$T_{eff} = \frac{T_{ttl} \times \Delta T}{PRT}, \tag{1}$$

as shown in Fig. 1c. The irradiation conditions were optimized in the following order: total irradiation time T_{ttl}, pulse duration ΔT, maximum sound pressure P_0, and ultrasound frequency f_0.

The LIPUS group underwent irradiation with ultrasound, while the control group did not. After irradiation, RNA was extracted from the LIPUS and control groups after 6-h incubation.

The maximum sound pressure P_0 was measured at depth d [m] from the transducer using a needle hydrophone (HY05N; Toray, Tokyo, Japan) on the central axis of the transducer. Ultrasound was irradiated to the hydrophone through the agar as well as the irradiation to cells. The sound field of a disk-type transducer is determined by D [11] and defined as

$$D = \frac{\lambda}{a^2} \cdot d, \tag{2}$$

where λ [m] is the wavelength and a [m] the radius of the transducer. Considering the theoretical sound pressure distribution [11] of a disk-type transducer [11], $D = 1.8$ was chosen to maintain the sound pressure difference between the center of the well and the edge of the well approximately twice as large. For each frequency f_0, the distance d was determined so that $D = 1.8$. Thus, distance d was set to 17 mm at 0.1 MHz, 35 mm at 0.3 MHz, 117 mm at 1 MHz, and 350 mm at 3 MHz, respectively.

To correctly evaluate pulse duration ΔT and acoustic energy, a polypropylene cylinder whose material is close to the acoustic impedance of the plate was bonded to the back of the plate to suppress multiple reflections within the plate, which was made of polystyrene, whose acoustic impedance was 2.52×10^6 kg/(m·s²), and the polypropylene cylinder had an acoustic impedance of 1.9×10^6 kg/(m·s²) [12]. To suppress the reflected waves from the bottom surfaces of the polypropylene cylinder and constant-temperature bath, the bottom surface of the polypropylene cylinder was roughened with sandpaper. The reflection coefficient for a rough surface is generally known to be lower compared with that for a flat surface [13].

Fig. 1 **a** Cross-sectional view of the experimental system for ultrasonic irradiation. **b** Schematic diagram of the transmitted waveform. **c** Effective irradiation time T_{eff}. **d** A new index P_N, showing the product of power and the total number of irradiation cycles
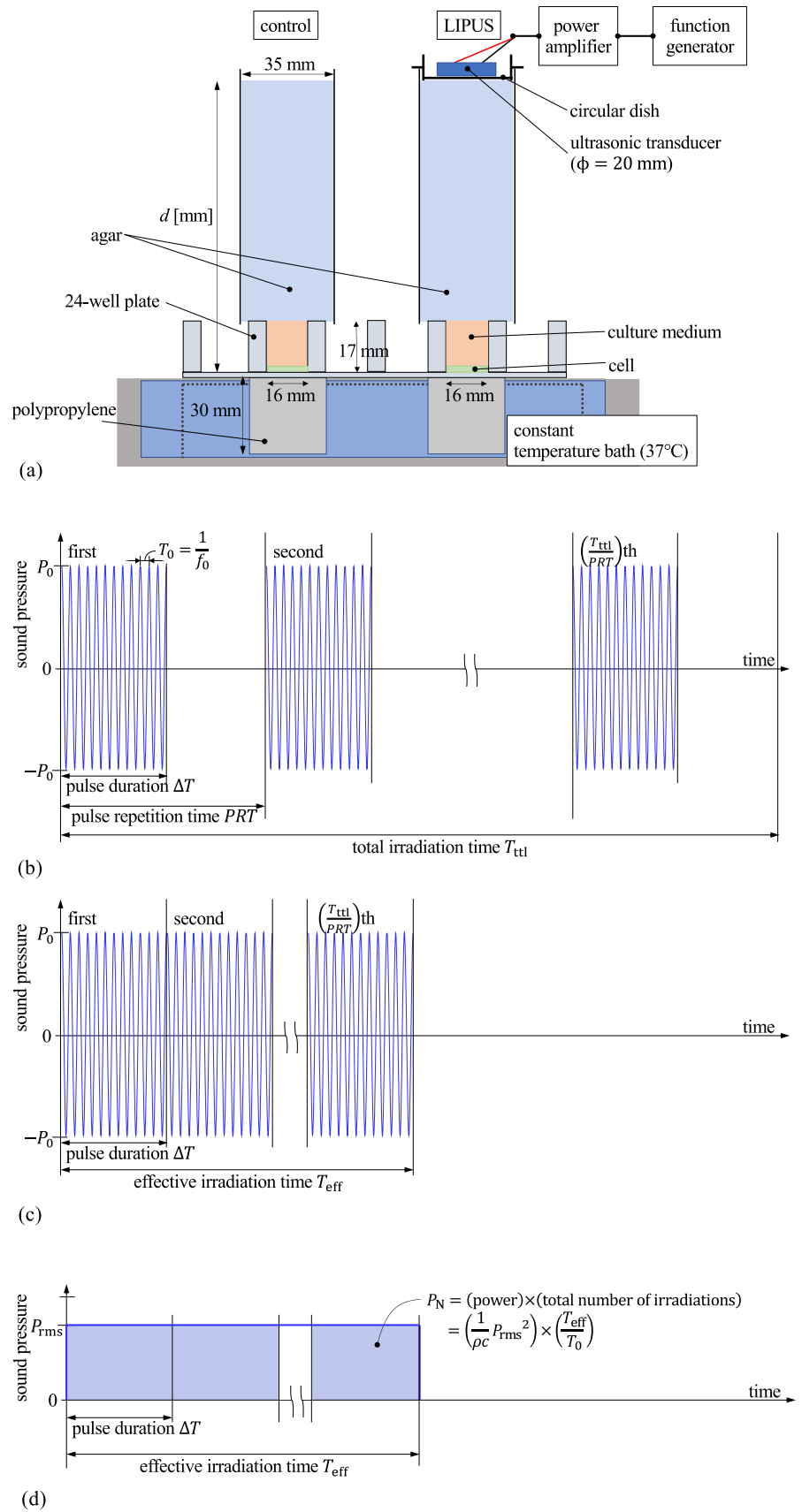
Evaluation of LIPUS-induced effect

In a previous study, we demonstrated that LIPUS therapy enhances the proliferation of human umbilical vein endothelial cells (HUVECs) in scratch assays [8]. LIPUS therapy also upregulates both mRNA expression and protein enhancement of eNOS [8]. It is well known that nitric oxide (NO) is produced by eNOS [14–16].

In the present study, it was necessary to examine numerous LIPUS irradiation conditions on in vitro HCAEC to determine the suboptimal LIPUS irradiation conditions. Therefore, only the mRNA expression of eNOS, a key molecule that promotes angiogenesis, was used as an evaluation index.

Real-time polymerase chain reaction

The procedures and conditions for the real-time polymerase chain reaction (PCR) were the same as those used in our previous study [8]. We extracted mRNA using the RNeasy Plus Mini kit (QIAGEN, Hilden, Germany) and QIAcube (QIAGEN, Hilden, Germany). Synthesis of cDNA was carried out using PrimeScript RT Master Mix (Takara Bio Inc., Shiga, Japan). The primer sequences (forward, reverse) were 5'-AAAGACAAGGCAGCAGTGGAAAT-3' and 5'-TCCACGATGGTGACTTTGGCTA-3' for eNOS, and 5'-GCACCGTCAAGGCTGAGAAC-3' and 5'-TGGTGAAGACGCCAGTGGA-3' for glyceraldehyde 3-phosphate dehydrogenase (GAPDH), all of which were designed by the Perfect Real Time Support System (Takara Bio, Shiga, Japan). After reverse transcription, real-time PCR was performed using TB Green Premix Ex Taq II (Takara Bio, Shiga, Japan), a CFX96TM Real-Time system (Bio-Rad Laboratories, California, USA), and a C1000TM Thermal Cycler (Bio-Rad Laboratories, California, USA).

The amplification efficiency of the PCR reaction greatly depends on the differences in each sample; therefore, it was necessary to normalize using the endogenous control gene, GAPDH, for this study. In the present study, the mRNA expression of eNOS, EX, was normalized to that of GAPDH and compared between the control and LIPUS groups. Parameters were compared between the control and LIPUS groups using an uncorrelated Student's t-test, and values of $P < 0.05$ were considered statistically significant.

Ultrasound evaluation index

The instantaneous intensity of the ultrasound, $I(t)$, is calculated as follows:

$$I(t) = \frac{p^2(t)}{\rho c}, \tag{3}$$

where $p(t) = P_0 \sin(2\pi f_0 t)$ is the instantaneous sound pressure, ρ is the density of the medium, and c is the sound velocity. The average intensity within the pulse repetition time PRT, I_{spta} [mW/cm^2], is a safety standard for diagnostic ultrasound systems [17] and is calculated by

$$I_{spta} = \frac{1}{PRT}\int_0^{PRT} I(t)dt = \frac{1}{PRT} \cdot \frac{1}{\rho c}\int_0^{\Delta T} p(t)^2 dt \approx \frac{1}{\rho c}\left(\frac{P_0}{\sqrt{2}}\right)^2 \frac{\Delta T}{PRT}. \tag{4}$$

To examine the action of ultrasound on cells that contributes to eNOS, EX expression, we defined the following two evaluation indices. First, the total energy per unit area, E_{ttl} [J/m^2], irradiated on the cells can be defined as the average intensity I_{spta} within the pulse repetition time PRT multiplied by the total irradiation time T_{ttl}:

$$E_{ttl} = I_{spta} \times T_{ttl} \approx \frac{1}{\rho c}\left(\frac{P_0}{\sqrt{2}}\right)^2 \frac{\Delta T}{PRT} \times T_{ttl} = \frac{1}{\rho c}\left(P_{rms}\right)^2 \cdot T_{eff}, \tag{5}$$

where P_{rms} is the root-mean-square value of $p(t)$ defined by

$$P_{rms} = \frac{P_0}{\sqrt{2}}. \tag{6}$$

We defined $\overline{E_{ttl}}$ by spatially averaging E_{ttl} over the irradiated area as follows:

$$\overline{E_{ttl}} = \begin{cases} 0.55 \times E_{ttl}, & \text{for } f = 0.1 \text{ or } 0.3\,\text{MHz} \\ 0.51 \times E_{ttl}. & \text{for } f = 1 \text{ or } 3\,\text{MHz} \end{cases} \tag{7}$$

When the total irradiation time T_{ttl}, pulse duration ΔT, maximum sound pressure P_0, and pulse repetition time PRT were kept constant, E_{ttl} did not change at various frequencies of f_0. Although conditions (1), (2), (3), (4), (11), (18), and (19) in Table 1 have nearly the same $\overline{E_{ttl}}$ value, the eNOS expression EX values were different, as shown in "Results".

Next, we introduced a new index P_N [J/(m$^2 \cdot \mu$s)] by calculating

$$P_N = E_{ttl} \times f_0 = I_{spta} \times T_{ttl} \times f_0 \approx \frac{1}{\rho c}\left(P_{rms}\right)^2\left(\frac{T_{eff}}{T_0}\right), \tag{8}$$

where $T_0 = 1/f_0$ is one period of ultrasound irradiation. $\overline{P_N}$ was defined by spatially averaging P_N over the irradiated area as follows:

$$\overline{P_N} = \begin{cases} 0.55 \times P_N, & \text{for } f = 0.1 \text{ or } 0.3\,\text{MHz} \\ 0.51 \times P_N. & \text{for } f = 1 \text{ or } 3\,\text{MHz} \end{cases} \tag{9}$$

E_{ttl} corresponds to the energy that changes to heat, and does not depend on the irradiation frequency f_0. Alternatively, to evaluate the mechanotransduction caused by ultrasonic irradiation, P_N shows the power per unit area, $\left(P_{rms}\right)^2/\rho c$, multiplied by the total number of irradiation cycles, T_{eff}/T_0, during the effective irradiation time T_{eff}, as shown in Fig. 1d.

Table 1 Irradiation condition of LIPUS, indices, and mRNA of eNOS for each experiment

Number	Ultrasound frequency $f_0 = \frac{1}{T_0}$ [MHz]	Maximum sound pressure P_0 [kPa]	Total irradiation time T_{ttl} [min]	Pulse duration ΔT [μs]	Pulse repetition time PRT [μs]	Wave cycle $wl = \Delta T \cdot f_0$ [cycles]	Duty cycle $DC = \frac{\Delta T}{PRT}$ [%]	Effective irradiation time $T_{\mathrm{eff}} = \frac{T_{\mathrm{ttl}} \cdot \Delta T}{PRT}$ [s]	Mechanical index MI	Average intensity I_{spta} [mW/cm²]	$\overline{E_{\mathrm{ttl}}}$ (×10⁶) [J/m²]	$\overline{P_{\mathrm{N}}}$ (×10⁶) [J/(m²·μs)]	mRNA of eNOS (/GAPDH) EX	$\widehat{EX}$ of Eq. (A10)
(1)	0.1	500	20	50	333	5	15	180	1.581	1231	8.1	0.8	1.05 ± 0.08	1.02
(2)	0.1	500	20	480	3200	48	15	180	1.581	1231	8.1	0.8	1.03 ± 0.13	1.02
(3)	0.3	500	20	46.7	311	14	15	180	0.913	1231	8.1	2.4	1.14 ± 0.09	1.12
(4)	0.3	500	20	160	1067	48	15	180	0.913	1231	8.1	2.4	1.19 ± 0.10	1.12
(5)	1	125	20	48	320	48	15	180	0.125	76.91	0.5	0.5	0.98 ± 0.10	0.97
(6)	1	250	20	48	320	48	15	180	0.25	307.6	1.9	1.9	1.01 ± 0.06	1.10
(7)	1	500	5	32	320	32	10	30	0.5	820.4	1.3	1.3	1.09 ± 0.15	1.06
(8)	1	500	20	16	320	16	5	60	0.5	410.2	2.5	2.5	1.15 ± 0.07	1.13
(9)	1	500	10	32	320	32	10	60	0.5	820.4	2.5	2.5	1.10 ± 0.11	1.13
(10)	1	500	20	32	320	32	10	120	0.5	820.4	5.0	5.0	1.20 ± 0.07	1.19
(11)	1	500	20	48	320	48	15	180	0.5	1231	7.6	7.6	1.20 ± 0.14	1.18
(12)	1	500	20	64	320	64	20	240	0.5	1641	10.1	10.1	1.19 ± 0.17	1.15
(13)	1	500	30	48	320	48	15	270	0.5	1231	11.3	11.3	1.18 ± 0.22	1.13
(14)	1	500	20	128	320	128	40	480	0.5	3282	20.2	20.2	1.00 ± 0.08	1.06
(15)	1	750	20	48	320	48	15	180	0.75	2769	17.0	17.0	1.13 ± 0.18	1.08
(16)	1	1000	20	48	320	48	15	180	1	4922	30.2	30.2	1.07 ± 0.09	1.01
(17)	1	1250	20	48	320	48	15	180	1.25	7691	47.3	47.3	0.97 ± 0.13	0.96
(18)	3	500	20	16	107	48	15	180	0.289	1231	7.6	22.7	1.05 ± 0.12	1.05
(19)	3	500	20	48	320	144	15	180	0.289	1231	7.6	22.7	1.02 ± 0.13	1.05

Using the indices, $\overline{E_{ttl}}$ and $\overline{P_N}$, we attempted to uniformly show the ultrasound contribution to eNOS expression, *EX*, for various values of five parameters under different irradiation conditions.

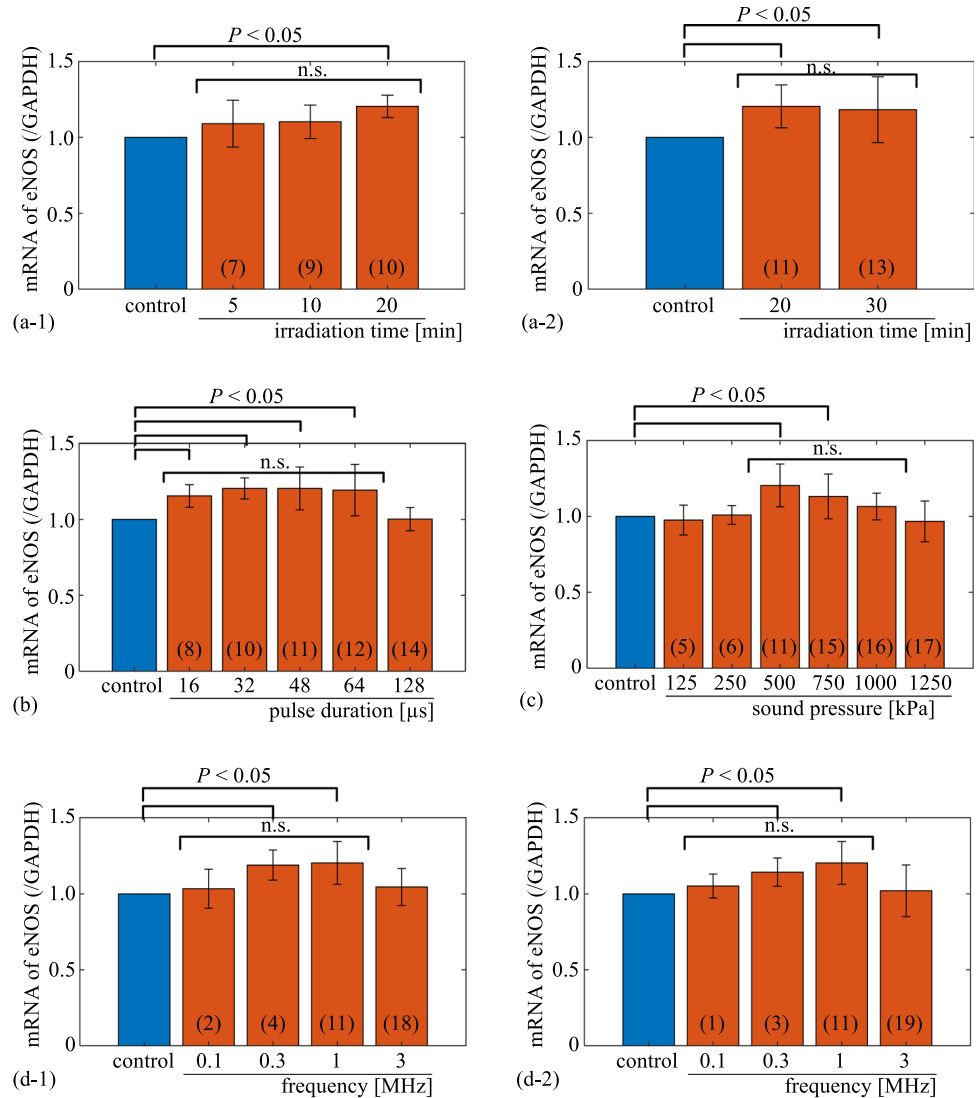## Results

In vitro experimental results

For various values of ultrasound total irradiation time T_{ttl}

The common irradiation conditions were set as follows: ultrasound frequency $f_0 = 1$ MHz, maximum sound pressure $P_0 = 500$ kPa, pulse duration $\Delta T = 32$ μs, and pulse repetition time $PRT = 320$ μs. Figure 2a-1 shows the results when the total irradiation time T_{ttl} was set to 5, 10, and 20 min, which correspond to (7), (9), and (10) in Table 1, respectively. When T_{ttl} was 20 min, the mRNA expression of eNOS, *EX*, was significantly higher ($P < 0.05$) than those of the control group.

For the common irradiation conditions of $f_0 = 1$ MHz, $P_0 = 500$ kPa, $\Delta T = 48$ μs, and $PRT = 320$ μs, T_{ttl} was set as 20 and 30 min, which correspond to (11) and (13) in Table 1, respectively. As shown in Fig. 2a-2, the mRNA expressions of eNOS, *EX*, increased significantly ($P < 0.05$) at 20 and 30 min compared to that in the control, while there was no significant difference between 20 and 30 min, and the expression of *EX* peaked at 20 min. Thus, a total irradiation time of $\widehat{T_{ttl}} = 20$ min was selected based on the clinical consideration that maintaining a fixed posture for more than 20 min places a burden on the patient.

Fig. 2 Expression of eNOS, *EX*, under different experimental conditions. **a** For various values of irradiation time T_{ttl}, (**a**-1) pulse duration $\Delta T = 32$ μs, and (**a**-2) $\Delta T = 48$ μs. **b** For various values of pulse duration ΔT. **c** For various values of maximum sound pressure P_0. **d** For various values of ultrasonic frequency f_0, (**d**-1) *wl* was fixed at 48 cycles, and (**d**-2) ΔT was fixed at 48 μs. The number in each bar corresponds to the number in Table 1. eNOS, endothelial nitric oxide synthase

For various values of pulse duration ΔT

Figure 2b shows the results obtained when the pulse duration ΔT was changed to 16, 32, 48, 64, and 128 µs, corresponding to (8), (10), (11), (12), and (14) in Table 1, respectively. The other irradiation conditions were identical to those described above: $f_0 = 1$ MHz, $P_0 = 500$ kPa, $T_{ttl} = 20$ min, and $PRT = 320$ µs. The expression EX was significantly ($P < 0.05$) increased at $\Delta T = 16$, 32, 48, and 64 µs compared to the control group, and there was no significant difference among $\Delta T = 16$, 32, 48, and 64 µs. For $\Delta T = 48$ µs, the expression EX significantly increased by 15% and then peaked. Based on these results, the optimal wave duration $\widehat{\Delta T} = 48$ µs was selected.

For various values of maximum sound pressure P_0

Figure 2(c) shows the results when the maximum sound pressures P_0 were 125, 250, 500, 750, 1000, and 1250 kPa, corresponding to (5), (6), (11), (15), (16), and (17) in Table 1, respectively. The other irradiation conditions were identical to those described above: $f_0 = 1$ MHz, $T_{ttl} = 20$ min, $\Delta T = 48$ µs, and $PRT = 320$ µs. The maximum sound pressure P_0 significantly ($P < 0.05$) increased the expression EX at 500 and 750 kPa compared to the control, with no significant difference between them, and the expression EX peaked at 500 kPa. Based on these results, an optimal sound pressure of $\widehat{P_0} = 500$ kPa was selected.

For various values of ultrasound frequency f_0

Figure 2d-1 shows the results obtained when the frequency f_0 was varied as 0.1, 0.3, 1, and 3 MHz, corresponding to (2), (4), (11), and (18) in Table 1, respectively. The other irradiation conditions were identical to those described above: $P_0 = 500$ kPa, $T_{ttl} = 20$ min, $PRT = 320$ µs, and $wl = 48$ cycles. When the wave cycle wl was fixed at 48 cycles, the pulse duration $\Delta T = wl/f_0$ changed according to the frequency f_0. The expression EX was significantly ($P < 0.05$) increased when the frequency f_0 was 300 kHz or 1 MHz compared with the control.

To change frequency f_0 with the same pulse duration ΔT, ΔT was fixed at 48 µs. The common irradiation conditions were as follows: $P_0 = 500$ kPa, $T_{ttl} = 20$ min, $\Delta T = 48 \pm 2$ µs, and $PRT = 320$ µs. Frequency f_0 was changed to 0.1, 0.3, 1, and 3 MHz, corresponding to (1), (3), (11), and (19) in Table 1, respectively. The results are shown in Fig. 2d-2. The expression EX increased significantly ($P < 0.05$) when f_0 was 300 kHz and 1 MHz compared with the control. Based on these results, the optimal frequency of $\widehat{f_0} = 1$ MHz was selected.
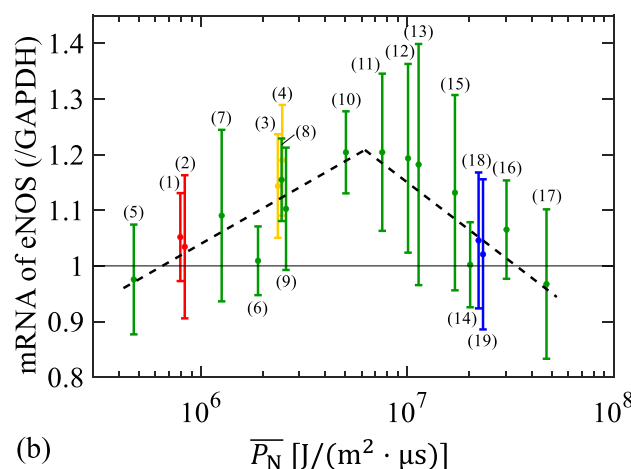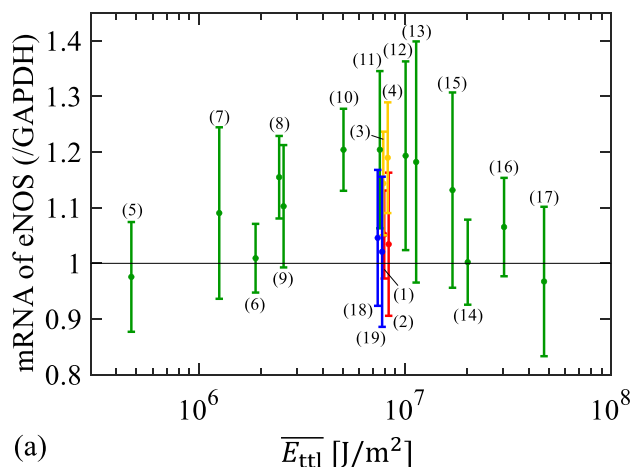

Fig. 3 a The relationship between energy index $\overline{E_{ttl}}$ and mRNA expression of eNOS, EX. **b** The relationship between the proposed index $\overline{P_N}$ (product of power and the total number of irradiation cycles) and EX

For indices E_{ttl} and P_N contributing to eNOS, EX expression

To examine the effects of ultrasound on cells that contribute to eNOS, EX expression, based on the above results, we evaluated the relationship between $\overline{E_{ttl}}$, $\overline{P_N}$, and EX for (1) to (19), as presented in Table 1. The results pertaining to $\overline{E_{ttl}}$ and $\overline{P_N}$ are shown in Fig. 3a and b, respectively. For f_0 of 0.1, 0.3, 1, and 3 MHz, the displayed colors were red, yellow, green, and blue, respectively.

Figure. 3a does not uniformly show the experimental eNOS expression for various values of five parameters under different irradiation conditions. Alternatively, Fig. 3b shows the eNOS mRNA expression, EX, and the approximated broken line graph (polyline) determined by the least squares fitting, which is described in the

Appendix. The broken line reached the maximum around $\overline{P_{\text{N\_max}}} = 6.2 \times 10^6$ J/(m$^2 \cdot$ μs), and the expression EX decreased as $\overline{P_{\text{N}}}$ moved away from this maximum.

Discussion

Based on these results, the suboptimal ultrasound irradiation conditions were determined as follows: frequency $\hat{f}_0 = 1$ MHz, maximum sound pressure $\widehat{P_0} = 500$ kPa, total irradiation time $\widehat{T_{\text{ttl}}} = 20$ min, pulse duration $\widehat{\Delta T} = 32 - 48$ μs, and pulse repetition rate $\widehat{PRT} = 320 \cdot$ μs.

As shown in Fig. 3b, the relationship between $\overline{P_{\text{N}}}$ and the mRNA expressions of eNOS, EX, showed an upward convex trend. When $\overline{P_{\text{N}}}$ was smaller than $\overline{P_{\text{N\_max}}}$ and under the conditions where EX was maximal, maximum sound pressure P_0 and the total number T_{eff}/T_0 of irradiation cycles were underestimated, and EX was not sufficiently enhanced, because P_{N} is the product of the power per unit area, $(P_{\text{rms}})^2/\rho c$, and the total number of irradiation cycles, T_{eff}/T_0.

However, for a P_{N} larger than $\overline{P_{\text{N\_max}}}$, I_{spta} or the total number T_{eff}/T_0 of irradiation cycles tended to be larger, and therefore, cell injury would be induced and EX was not enhanced.

Caveolae in endothelial cells reportedly play an important role in detecting strain and stress on the extracellular membrane via β1-integrin and contributing to the associated signal transduction [18–22]. When cells are irradiated by ultrasound, caveolae are displaced and velocity is generated. The evaluation index P_{N} in Eq. (8) includes the power and total number of irradiation cycles, showing that the amplitude and number of actuations on the caveolae are important for eNOS, EX expression. Therefore, these results indicate that LIPUS treatment may be more efficient under conditions with an extended evaluation index P_{N} within a range that does not cause cell damage when setting ultrasound irradiation conditions.

Study limitations

The present study had several limitations. First, because the suboptimum irradiation conditions were determined in the order of total irradiation time T_{ttl}, pulse duration ΔT, maximum sound pressure P_0, and frequency f_0, the optimum is apparent but not real. Thus, it is possible that there were more efficient conditions than those determined in this study. It remains to be confirmed whether cellular damage is caused by ultrasound irradiation under conditions of large I_{spta} values and a mechanical index $MI = P_{\text{neg}}/\sqrt{f_0}$, where P_{neg} is the maximum negative pressure, showing an evaluation index of

ultrasound effects on a living body [23]. The LIPUS was irradiated under only two conditions for frequencies f_0 of 0.1, 0.3, and 3 MHz. It is necessary to confirm the relationship between $\overline{P_{\text{N}}}$ and the mRNA expressions of eNOS, EX, with a frequency f_0 other than 1 MHz.

In the present study, the mRNA expressions of eNOS, EX, decreased for a P_{N} larger than $\overline{P_{\text{N\_max}}}$. This could be attributed to cell damage caused by irradiating ultrasound. Therefore, in our future studies, the proper maximum sound pressure P_0 and the total number T_{eff}/T_0 will be determined by evaluating the cell injury.

Conclusion

The present study determined the suboptimal ultrasound irradiation conditions that would promote the expression of eNOS, EX, in HCAEC. The suboptimal irradiation conditions were as follows: ultrasound frequency, $\hat{f}_0 = 1$ MHz; maximum sound pressure, $\widehat{P_0} = 500$ kPa; total irradiation time, $\widehat{T_{\text{ttl}}} = 20$ min; pulse duration, $\widehat{\Delta T} = 48$ μs; and pulse repetition time, $\widehat{PRT} = 320$ μs. An upward convex trend was observed between P_{N} and the mRNA expression of eNOS, EX, suggesting that they may be influenced by the proposed evaluation index P_{N}, calculated as the product of power and the total number of irradiation cycles applied to cells using LIPUS.

Appendix: Derivation of approximated lines in Fig. 3b using the least squares method

By introducing new variables x and y as

$$x = \log_{10}\overline{E_{\text{q}}}, \tag{A1}$$

$$y = EX, \tag{A2}$$

let us define an approximated line graph (polyline) in Fig. 3b as

$$y = \begin{cases} a_1(x - x_0) + y_0, & (x < x_0) \\ a_2(x - x_0) + y_0, & (x \geq x_0), \end{cases} \tag{A3}$$

where a_1, a_2, x_0, and y_0 are the coefficients of the approximated polyline that should be estimated. For the measured values $\{x_i, y_i\}$ $(x_i < x_0)$ and $\{x_j, y_j\}$ $(x_j \geq x_0)$, the weighted mean squared error $\alpha(a_1, a_2, y_0; x_0)$ between the measured values and polyline in Eq. (A3) can be obtained as follows:

$$\alpha(a_1, a_2, y_0; x_0) = \sum_i w_i \cdot \left| y_i - (a_1(x_i - x_0) + y_0) \right|^2$$
$$+ \sum_j w_j \cdot \left| y_j - (a_2(x_j - x_0) + y_0) \right|^2, (x_i < x_0, x_j \geq x_0) \tag{A4}$$

where w is the weight defined by the variance of EX, σ^2, as

$$w = \frac{1}{\sigma^2}, \tag{A5}$$

where the standard deviation σ of EX is presented in Table 1 and Fig. 3b. By fixing the coefficient x_0 to an arbitrary value and defining x' as

$$x'(x_0) = x - x_0, \tag{A6}$$

the condition minimizing $\alpha(a_1, a_2, y_0; x_0)$ is given by

$$\frac{1}{2}\frac{\partial \alpha(a_1, a_2, y_0; x_0)}{\partial a_1} = a_1 \sum_i w_i x_i'(x_0)^2 - \sum_i w_i y_i x_i'(x_0) + y_0 \sum_i w_i x_i'(x_0) = 0, \tag{A7}$$

$$\frac{1}{2}\frac{\partial \alpha(a_1, a_2, y_0; x_0)}{\partial a_2} = a_2 \sum_j w_j x_j'(x_0)^2 - \sum_j w_j y_j x_j'(x_0) + y_0 \sum_j w_j x_j'(x_0) = 0, \tag{A8}$$

$$\frac{1}{2}\frac{\partial \alpha(a_1, a_2, y_0; x_0)}{\partial y_0} = y_0 \left(\sum_i w_i + \sum_j w_j \right) - \left(\sum_i w_i y_i + \sum_j w_j y_j \right) + a_1 \sum_i w_i x_i'(x_0) + a_2 \sum_j w_j x_j'(x_0) = 0. \tag{A9}$$

By substituting a_1 into Eq. (A7), and a_2 in Eq. (A8) into Eq. (A9), $\widehat{y_0}(x_0)$, which minimizes $\alpha(a_1, a_2, y_0; x_0)$ with fixed x_0, is estimated by

$$\widehat{y_0}(x_0) = \frac{B_I E_I D_J + B_J E_J D_I - \left(\sum_i w_i y_i + \sum_j w_j y_j \right) D_I D_J}{B_I^2 D_J + B_J^2 D_I - \left(\sum_i w_i + \sum_j w_j \right) D_I D_J}, \tag{A10}$$

where

$$B_I = \sum_i w_i x_i'(x_0), B_J = \sum_j w_j x_j'(x_0),$$
$$D_I = \sum_i w_i x_i'(x_0)^2, D_J = \sum_j w_j x_j'(x_0)^2, \tag{A11}$$
$$E_I = \sum_i w_i y_i x_i'(x_0), E_J = \sum_j w_j y_j x_j'(x_0).$$

Subsequently, $\widehat{a_1}(x_0)$ and $\widehat{a_2}(x_0)$ minimizing $\alpha(a_1, a_2, y_0; x_0)$ with a fixed x_0 are estimated by substituting Eq. (A10) into Eq. (A7) and (A8), respectively.

$$\widehat{a_1}(x_0) = \frac{E_I - B_I \widehat{y_0}(x_0)}{D_I}, \tag{A12}$$

$$\widehat{a_2}(x_0) = \frac{E_J - B_J \widehat{y_0}(x_0)}{D_J}. \tag{A13}$$

Using $\widehat{a_1}(x_0)$, $\widehat{a_2}(x_0)$, and $\widehat{y_0}(x_0)$, $\alpha(\widehat{a_1}(x_0), \widehat{a_2}(x_0), \widehat{y_0}(x_0); x_0)$ is calculated for each of the various values $\{x_0\}$. Thus, the coefficient $\widehat{x_0}$ that minimizes $\alpha(a_1, a_2, y_0; x_0)$ in Eq. (A4) can be obtained as follows:

$$\widehat{x_0} = \underset{x_0}{\mathrm{argmin}}\, \alpha(\widehat{a_1}(x_0), \widehat{a_2}(x_0), \widehat{y_0}(x_0); x_0). \tag{A14}$$

Finally, the optimum values of a_1, a_2, and y_0 for the minimum condition can be determined by $\widehat{a_1}(\widehat{x_0})$, $\widehat{a_2}(\widehat{x_0})$, and $\widehat{y_0}(\widehat{x_0})$, respectively.

Declarations

Conflict of interest Daiki Ouchi, Shohei Mori, Mototaka Arakawa, Tomohiko Shindo, Hiroaki Shimokawa, Satoshi Yasuda, and Hiroshi Kanai declare no conflicts of interest.

Ethical approval None.

References

1. Moran AE, Forouzanfar MH, Roth GA, et al. Temporal trends in ischemic heart disease mortality in 21 world regions, 1980 to 2010: the global burden of disease 2010 study. Circulation. 2014;129:1483–92.
2. Hata J, Kiyohara Y. Epidemiology of stroke and coronary artery disease in Asia. Circ J. 2013;77:1923–32.
3. Haar G. Therapeutic applications of ultrasound. Prog Biophys Mol Biol. 2007;93:111–29.
4. Hanawa K, Ito K, Aizawa K, Shindo T, et al. Low-intensity pulsed ultrasound induces angiogenesis and ameliorates left ventricular dysfunction in a porcine model of chronic myocardial ischemia. PLoS ONE. 2014;9:e104863.
5. Albornoz PM, Khanna A, Longo UG, et al. The evidence of low-intensity pulsed ultrasound for in vitro, animal and human fracture healing. Br Med Bull. 2011;100:39–57.
6. Tanaka E, Kuroda S, Horiuchi S, et al. Low-intensity pulsed ultrasound in dentofacial tissue engineering. Ann Biomed Eng. 2015;43:871–86.
7. Yang FY, Lu WW, Lin WT, et al. Enhancement of neurotrophic factors in astrocyte for neuroprotective effects in brain disorders using low-intensity pulsed ultrasound stimulation. Brain Stimul. 2015;8:465–73.
8. Shindo T, Ito K, Ogata T, et al. Low-intensity pulsed ultrasound enhances angiogenesis and ameliorates left ventricular dysfunction in a mouse model of acute myocardial infarction. Arterioscler Thromb Vasc Biol. 2016;36:1220–9.
9. Parton RG. Life without caveolae. Science. 2001;293:2404–5.
10. Parton RG, Pozo MA. Caveolae as plasma membrane sensors, protectors and organizers. Nat Rev Mol Cell Biol. 2013;14:98–112.
11. Bass R. Diffraction effects in the ultrasonic field of a piston source. J Acoust Soc Am. 1958;30:602–5.
12. Lochab J, Singh VR. Acoustic behaviour of plastics for medical applications. IJPAP. 2004;42:595–9.
13. Wilhjelm JE, Pedersen PC, Jacobsen SM. The influence of roughness, angle, range, and transducer type on the echo signal from planar interfaces. IEEE Trans Ultrason Ferroelectr Freq Control. 2001;48:511–21.
14. Dimmeler S, Fleming I, Fisslthaler B, et al. Activation of nitric oxide synthase in endothelial cells by Akt-dependent phosphorylation. Nature. 1999;399:601–5.
15. Lowry JL, Brovkovych V, Zhang Y, et al. Endothelial nitric-oxide synthase activation generates an inducible nitric-oxide

synthase-like output of nitric oxide in inflamed endothelium. J Biol Chem. 2013;288:4174–93.

16. Vanhoutte PM, Zhao Y, Xu A, et al. Thirty years of saying NO: sources, fate, actions, and misfortunes of the endothelium-derived vasodilator mediator. Circ Res. 2016;119:375–96.

17. Nelson TR, Fowlkes JB, Abramowicz JS, et al. Ultrasound biosafety considerations for the practicing sonographer and sonologist. J Ultrasound Med. 2009;28:139–50.

18. Yu J, Bergaya S, Murata T, et al. Direct evidence for the role of caveolin-1 and caveolae in mechanotransduction and remodeling of blood vessels. J Clin Invest. 2006;116:1284–91.

19. Pozo MA, Balasubramanian N, Alderson NB, et al. Phospho-caveolin-1 mediates integrin-regulated membrane domain internalization. Nat Cell Biol. 2005;7:901–8.

20. Jokhadar SZ, Majhenc J, Svetina S, et al. Positioning of integrin β1, caveolin-1, and focal adhesion kinase on the adhered membrane of spreading cells. Cell Biol Int. 2013;37:1276–84.

21. Yeo MG, Oh HJ, Cho HS, et al. Phosphorylation of Ser 21 in Fyn regulates its kinase activity, focal adhesion targeting, and is required for cell migration. J Cell Physiol. 2011;226:236–47.

22. Gervásio OL, Phillips WD, Cole L, et al. Caveolae respond to cell stretch and contribute to stretch-induced signaling. J Cell Sci. 2011;124:3581–90.

23. Patterson B, Miller DL. Experimental measurements of ultrasound attenuation in human chest wall and assessment of the mechanical index for lung ultrasound. Ultrasound Med Biol. 2020;46:1442–54.